Modeling and Simulation of Triclosan Kinetics and Distribution in Humans Using PBPK Model

Vincenza Cascella[1], Monica Andreassen[2], Trine Husøy[2], Hubert Dirven[2], Bernt Lie[1]

[1]University of South-Eastern Norway, Bernt.Lie@usn.no;
[2]Department of Toxicology and Risk Assessment; Norwegian Institute of Public Health

Abstract

Triclosan (TCS) has been used as an antibacterial additive in several personal care products (PCPs) for more than 40 years. In animals studies, it is observed that TCS in rats has adverse effects on the endocrine function and thyroid hormone homeostasis, and intensify antibiotic resistance. In human studies, significant levels of TCS are detected in human plasma and breast milk. In this study, a Physiologically Based Pharmacokinetic or Toxicokinetic (PBPK/TK) model is developed to describe the concentration of triclosan in human organs after exposure through the skin (dermal) or orally. Several studies have been conducted on toxicokinetics of TCS, but there is a lack of information on parameters for PBPK models. In this paper, focus is on finding parameters for TCS to be used in the PBPK model. In a first case, the PBPK model was based on data for TCS and the structurally related chemical Bisphenol A (BPA), in a second case, partition coefficients were found using Poulin's method. The simulations were carried out using MATLAB, and the results for the two cases are compared.

Keywords: Triclosan, PBPK, Model parameters

1 Introduction

In everyday life people are surrounded by products which contain chemicals that might have negative effects on the human body. Many chemical compounds can be intentionally or unintentionally inhaled, ingested, or dermally absorbed. Various risks that could incur upon exposure are investigated (Fang et al., 2010). In animals studies, it is observed that *triclosan* (TCS) in rats has adverse effects on the endocrine function and thyroid hormone homeostasis, and intensify antibiotic resistance. The widespread application of TCS in numerous personal care and household products such as disinfectants, soaps, detergents, toothpastes, mouthwashes, fabrics, deodorants, shampoo, plastic additives in addition to several veterinary and industrial products (Dann and Hontela, 2011), has led to concerns regarding human health risks (Vingskes and Spann, 2018). TCS, an organic compound categorized as a polychloro phenoxyphenol, is a chlorinated aromatic compound that has functional groups representative of both ethers and phenol. Invented more than 40 years ago, and used increasingly over the past 25 years, regulations were even-tually invoked in 2010 by the European Community Cosmetic Directive on the use of TCS, limiting the concentration of TCS at 0.1-0.3% of product weight in personal care products. This percentage is considered safe in everyday products defined as toothpaste, hand soaps, shower gels, and deodorants (Dann and Hontela, 2011). The effects of TCS as an environmental chemical is also of concern, but this is not considered further here.

Physiologically based pharmacokinetic (PBPK) modeling and simulation can be used to predict the pharmacokinetic behavior of drugs in humans using clinical data (Zhao et al., 2011). The purpose for developing a PBPK for TCS is the wide exposure to the substance and lack of information about its toxicity on long-term use. Another reason, not to be underestimated, is the reduction of experiments on animals, for ethical reasons. PBPK modeling is a quantitative attempt to model the drug distribution in the body in compartments and to predict tissue concentration within specific organs (liver, kidney), tissue (skin, muscle), and body fluids (blood, Cerebrospinal fluid (CSF) and urine).

Here, we report the absorption, distribution, metabolism and excretion (ADME) of TCS after exposure via the dermal and/or oral route. Section 2 gives an overview of the system, the dynamic model is presented in Section 3, simulation results are presented and discussed in Section 4, and some conclusions are drawn in Section 5.

2 System Overview

2.1 Organs and Topology

Organs, blood flow, topology, and intake of TCS is illustrated in Figure 1.

The model equations follow the principles of mass transport, fluid dynamics, and biochemistry in order to simulate the evolution of a substance in the body (Campbell et al., 2012). PBPK models can predict the timescales and concentration in which TCS appear and disappear from various organs of the body, for setting dosing guidelines and risk assessment. Each compartment is described by capillary blood flow and capillary-tissue volume, as well as partitioning between capillary-tissue.

Each tissue is defined with assumptions of either perfusion-rate-limited or permeability-rate-limited.
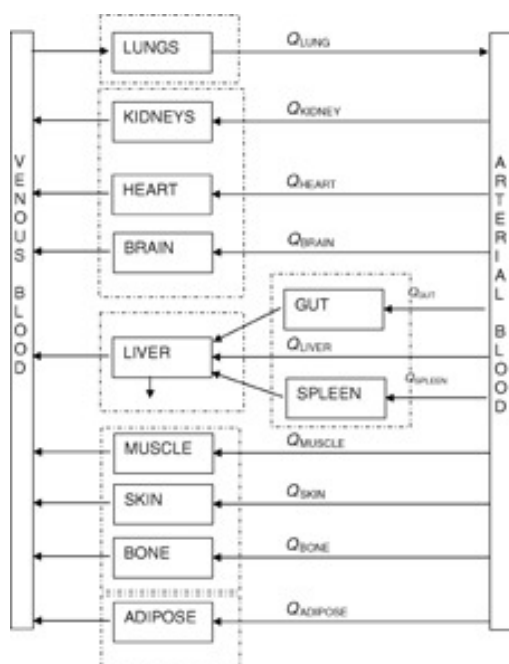
https://doi.org/10.3384/ecp18153148

148

Proceedings of The 59th Conference on Simulation and Modelling (SIMS 59), 26-28 September 2018, Oslo Metropolitan University, Norway

Figure 1. Flowchart of organ topology.

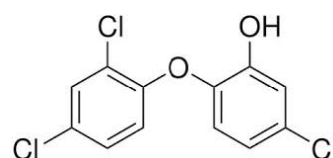**Figure 2.** Molecular structure of triclosan (TCS). From (Fang et al., 2010).
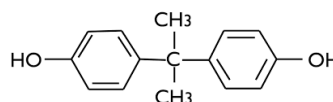
Figure 3. Molecular structure of bisphenol A (BPA).

Perfusion-rate- limited kinetics tends to exist for small lipophilic molecules where the blood flow to the tissue proved to be the limiting process of the absorption. Permeability-rate-limited kinetics occurs for more hydrophilic and larger molecules where the permeability across the cell membrane becomes the limiting process of absorption. (Zhuang and Lu, 2016).

2.2 Triclosan and Data

Triclosan is used as an anti-bacterial component in toothpaste, deodorant, etc. The anti-bacterial operation of Triclosan is as follows[1]. The cell membrane of bacteria is held together by a lipid bi-layer. In order for bacteria to live and grow, this lipid bi-layer must be able to grow. This growth takes place when a regulatory gene, named FabI, encodes an enzyme called enoyl-acyl carrier protein reductase (ENR) such that lipids can attach to the active site of ENR and then be inserted into the bi-layer. If Triclosan is present, Triclosan is instead adsorbed to the active site of ENR and blocks the uptake of lipids. This effectively blocks the growth of bacteria cells.

Triclosan has chemical formulae $C_{12}H_7Cl_3O_2$ (CAS[2] number 3380-34-5), with chemical structure as indicated in Fig. 2.

Triclosan is a colorless to off-white crystalline powder with a slightly aromatic odor, and is tasteless. Triclosan has low solubility in water (0.1 g/L) but much higher solubility in lipids (fatty acids). Physical-chemistry data for TCS are limited, and it may be necessary instead to use

data for structurally related molecules.

Bisphenol A (BPA; 2,2-bis(4-hydroxyphenyl)propane is a chemical compound found in many products (Konieczna et al., 2015), hence important data are readily available. BPA is an organic compound composed of two phenol rings connected by a methyl bridge, with two methyl functional groups attached to the bridge, Fig. 3.

BPA is structurally related molecule to TCS, Figures 2 and 3. Although they have differences, important properties such as the octanol/water coefficient are in the same range, Table 1.

In addition, major metabolism through sulphatation and glucuronidation is the same. It can be assumed that TCS and BPA have a comparable tendency of to be solubilized in tissue.

2.3 Triclosan Metabolism

Triclosan metabolizes to form conjugates *triclosan sulfate* and *triclosan glucuronide*, Fig. 4.

The operation of triclosan metabolism is as follows. A family of enzymes known as SULT (sulfotransferase) catalyze the transfer of a sulfonate group ($-SO_3^-$) from PAPS ($3'$-phosphoadenosine-$5'$-phosphosulfate) to triclosan, forming the conjugate *triclosan sulfate* with the release of PAP (3-phosphoadenosine-5-phosphate). Denoting triclosan by T and triclosan sulfate by T_S we can write the overall reaction as

$$PAPS + T \xrightarrow{SULT} T_S + PAP. \quad (1)$$
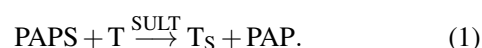
Similarly, an enzyme known as UGT (Uridine 5'-diphospho-glucuronosyl transferase = UDP-glucuronosyl transferase) catalyzes the transfer of the glucuronic acid

Table 1. Molecular mass (M_w) and *n*-octanol–water solubility parameter $\log K_{ow}$ for TCS and BPA. Taken from `https://chem.nlm.nih.gov/chemidplus/rn/3380-34-5` (TCS) and `https://chem.nlm.nih.gov/chemidplus/name/bisphenol` (BPA).

	TCS	BPA
M_w	289.53 g/mol	228.9 g/mol
$\log K_{ow}$	4.76	3.32

---

[1] `https://illumin.usc.edu/68/what-makes-antibacterial-soap-antibacterial/`
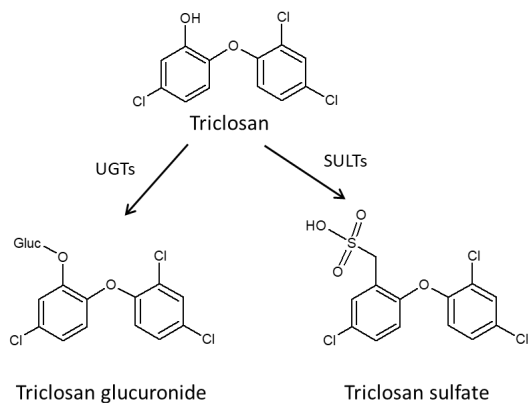
[2] Chemical Abstracts Service)

Figure 4. Metabolism of triclosan into glucuronides and sulfates. After (Fang et al., 2010).

component of UDP-glucuronic acid to triclosan, forming the conjugate triclosan glucuronide as well as a residual of UDP-glucuronic acid. Denoting UDP-glucuronic acid by G, the conjugate *triclosan glucuronide* by T_G, and the residual of UDP-glucuronic acid by $\bar{G}$, we can write the overall reaction as

$$G + T \xrightarrow{\text{UGT}} T_G + \bar{G}. \tag{2}$$
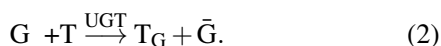
In both cases, triclosan (T, substrate) is adsorbed on the enzyme surface and covers/is inserted into the active site of the enzyme. Provided that triclosan has been adsorbed into the active site, we assume that a co-substrate (PAPS or G) also is adsorbed at the active site, forming a substrate/co-substrate complex. Next, a reaction takes place in this complex formed at the active site, and conjugated triclosan (T_S or T_G) is formed together with a co-product (PAP or $\bar{G}$) and these then desorb from the active site. Under the conditions of constant enzyme concentration and constant co-substrate concentration, the overall reaction rate referring to triclosan can be written as:

$$\hat{r}_j = \hat{r}_j^{\max} \frac{c_T}{c_T + K_T^j} \tag{3}$$

where $[\hat{r}_j]$ is given in mole/(time and protein mass), and $j \in \{S, G\}$. The individual reaction rates are thus:

$$\hat{r}_S = \hat{r}_S^{\max} \frac{c_T}{c_T + K_T^S} \tag{4}$$

$$\hat{r}_G = \hat{r}_G^{\max} \frac{c_T}{c_T + K_T^G}. \tag{5}$$

The conjugation of triclosan has been demonstrated in vitro in the human liver microsomes or cytosol (Wang et al., 2004), and the parameters taken from this study are shown in Table 2.

From Table 2 it should be observed that the molar rates of generation are given as

$$\dot{n}_j^g = \hat{r}_j \cdot m_{p,j} \tag{6}$$

Table 2. Michaelis-Menten reaction parameters for TCS metabolism in human liver (Wang et al., 2004).

	$K_T^j \left[\frac{\mu\text{mol}}{\text{L}}\right]$	$\hat{r}_j^{\max} \left[\frac{\text{pmol}}{\text{min mg Protein}}\right]$
Sulfonation	8.5 ± 3.2	95.9 ± 28.4
Glucuronidation	107 ± 22.2	739 ± 163

where $m_{p,j}$ is the relevant mass of protein in the liver. It should be noted that the available protein mass differs in sulfonation and glucuronidation: (Wang et al., 2004) indicate that sulfonation takes place in the human liver cytosol while glucuronidation takes place in the liver microsomes. Ideally, we would like to relate $m_{p,j}$ to the mass m_h of the liver (hepatic mass) as an organ instead, in other words to find ξ_j satisfying

$$m_{p,j} = \xi_j m_h. \tag{7}$$

In (Cubitt et al., 2009), the hepatic cytosolic scaling factor was found in the range $\xi_S^h \in [45, 134]$ mg protein in liver *cytosol* per g of liver, with a mean weighted value $\xi_S^h = 80.7 \times 10^{-3}$. They also report a typical fraction protein in intestine cytosol per g intestine to be $\xi_S^i = 18 \times 10^{-3}$. Observe that the rate numbers given in Table 2 do not necessarily carry over from liver to intestine.

In (Barter et al., 2007), experimental results are cited in the range $\xi_G^h \in [19, 77]$ mg protein in liver *microsomes* per g of liver. The value probably varies among individuals, with age, and by gender. A possible useful value may be $\xi_G^h = 30 \times 10^{-3}$.

2.4 Partition Coefficients

Most organs include blood flow with TCS through capillaries, and diffusion of TCS from the capillaries into the surrounding tissue. With capillary concentration $c_c(t)$ of the drug, the tissue concentration is $c_t'(t, x)$ — in a simplified description the tissue concentration is $c_t^*(t)$ at the interface, and $c_t(t)$ in the bulk of the tissue; $c_t = \lambda c_t^*$ where λ is the *partition coefficient* (PC). The driving force for diffusion is $\Delta c = c_c - c_t^*$. For organs where the tissue only interacts with the capillary, at equilibrium, $\Delta c_{eq} = 0$, thus $c_{t,eq} = \lambda c_{t,eq}^* = \lambda c_{c,eq}$. Accurate partition coefficients is important for getting realistic results.

Finding PCs from *in vivo* experiments takes time and is costly. Some progress has been made in developing correlation formulas for PCs, where the PC is correlated with knowledge of tissue and blood (capillary) composition in terms of neutrolipids, phospholipid, and water fractions. Results in general demonstrate that the correlation formulas can provide a good approximation for partition coefficients (Kuepfer et al., 2016). One such correlation expression is the algorithm of Poulin and Krishnan. Let S be the solubility in g solute per 100 g of solvent. Specifically, we consider the solubility of drug (TCS) in water S_w and drug in *n*-octanol S_o. The solubilities are taken to be proportional,

$$S_o = K_{ow} S_w. \tag{8}$$

Organ	λ BPA	λ TCS
Fat, fa	0.7	0.2536
Bone, bo	0.5	0.7392
Brain, br	4.4	1.2941
Kidney, ki	4.4	1.2774
Liver, li	5.7	1.2409
Lung, lu	5.5	1.3099
Muscle, mu	0.8	1.2446
Skin, ski	5.7	1.1174

Typically, $\log K_{ow}$ is given — here, we use $\log K_{ow} \approx 4.8$ (Fang et al., 2010). With $S_w = 10^{-3}$ at $25\,°C$, S_o is thus known.

Next, we assume that the drug is associated with neutral lipids (N), phospholipids (P), and water (W) in both tissue (t) and capillaries (blood, b). The fraction of these are denoted χ_j where $j \in \{N, P, W\}$; values for these fractions are found in (Ye et al., 2016) for each organ. By observing that at equilibrium,

$$\lambda = \frac{c_{t,eq}}{c_{c,eq}} = \frac{c_{t,eq}}{c_{b,eq}}, \tag{9}$$

an estimate of the PC can, e.g., be given as described in (Poulin and Krishnan, 1995a,b):

$$\lambda = \frac{\chi_{N,t}S_o + \chi_{P,t}(0.7S_w + 0.3S_o) + \chi_{W,t}S_w}{\chi_{N,b}S_o + \chi_{P,b}(0.7S_w + 0.3S_o) + \chi_{W,b}S_w}. \tag{10}$$

Here, it has been assumed that neutral lipids are insoluble in water, and that phospholipids are 70% soluble in water and 30% soluble in *n*-octanol.

Table 3 shows the PCs for BPA, compared to the PCs for TCS as found from Eq. 10.

3 Dynamic Model

3.1 General Balance

As pharmacokinetic models are used for assessing concentration of chemicals in different organism/tissue of a body, the mass balance equations are transferred into differential equations in the form of number of moles. The general species balance in molar form is

$$\frac{dn_j}{dt} = \dot{n}_j^i - \dot{n}_j^e + \dot{n}_j^g, \tag{11}$$

where:

n_j : number of moles of species j accumulated in the volume,

$\dot{n}_j^i$: influent in moles per unit time of species j,

$\dot{n}_j^e$: effluent flow in moles per unit time of species j,

$\dot{n}_j^g$: generated number of moles per time unit of species j.

3.2 Compartments

Organs are often represented by 2-compartment models consisting of capillary volume and tissue volume. Assuming well mixed volumes and not accumulation of blood, without metabolism, the two volumes can be described by

$$\frac{dc_c}{dt} = \frac{\dot{V}}{V_c}\left(c_c^i - c_c\right) - \frac{\Theta_{c2t}}{V_c}\left(c_c - c_t^*\right) \tag{12}$$

$$\frac{dc_t}{dt} = \frac{\Theta_{c2t}}{V_t}\left(c_c - c_t^*\right) \tag{13}$$

where $c_t = \lambda c_t^*$. Assuming that Θ_{c2t} is "small" (permeation limited),

$$c_c \approx c_c^i, \tag{14}$$

and the model reduces to

$$\frac{dc_t}{dt} = \frac{\Theta_{c2t}}{V_t}\left(c_c^i - \frac{1}{\lambda}c_t\right). \tag{15}$$

On the other hand, if Θ_{c2t} is "large" (perfusion limited), we will have a quasi steady state where

$$c_c \approx c_t^* = \frac{1}{\lambda}c_t, \tag{16}$$

thus

$$\frac{dc_c}{dt} = \frac{\dot{V}}{V_c}\left(c_c^i - c_c\right) \tag{17}$$

and $c_t = \lambda c_c$.

Four organs need special treatment: metabolism takes place in the skin (dermal uptake) and in the liver; for these, metabolism reactions must be included. Furthermore, the GI tract/the intestine (oral intake) or the skin (dermal intake) need to include a transport model for the drug. Finally, the kidney has an additional "leakage" of drug from the tissue to urine.

3.3 Non-metabolic Organs

Whether the system is permeation limited or perfusion limited (or a mixture), the models in Section 3.2 need to be applied to each of free triclosan, triclosan sulfate, and triclosan glucuronide.

3.4 Metabolic Organs

Free triclosan can metabolize (react) into its conjugates; the balances are:

$$\frac{dn_{T,k}}{dt} = \dot{V}\left(c_{T,k}^i - c_{T,k}^*\right) + \dot{n}_{T,k}^g + \dot{n}_{d2s} \tag{18}$$

$$\frac{dn_{TG,k}}{dt} = \dot{V}\left(c_{TG,k}^i - c_{TG,k}^*\right) + \dot{n}_{TG,k}^g \tag{19}$$

$$\frac{dn_{TS,k}}{dt} = \dot{V}\left(c_{TS,k}^i - c_{TS,k}^*\right) + \dot{n}_{TS,k}^g \tag{20}$$

Here, index k refers to the organ where metabolism takes place — either liver or skin. The term denoted $\dot{n}_{d2s}$ is the

quantity of triclosan applied on the skin or taken in orally[3]. Excretion is through the kidney in the urine, and can be expressed as:

$$\dot{n}_{j,\text{k2u}} = \Theta_{\text{k2u}} c^{*}_{j,\text{ins}} \tag{21}$$

3.5 Flow Junction

The flow topology has one junction at the inlet to the blood pool. For this junction, no mass is accumulated. Steady state species balances for this junction lead to:

$$\dot{n}^{\text{e}}_{k,\text{bp}} = \dot{n}^{\text{e}}_{k,\text{ins}} + \dot{n}^{\text{e}}_{k,\text{br}} + \dot{n}^{\text{e}}_{k,\text{mu}} + \dot{n}^{\text{e}}_{k,\text{sk}} + \dot{n}^{\text{e}}_{k,\text{ki}}$$
$$+ \dot{n}^{\text{e}}_{k,\text{bo}} + \dot{n}^{\text{e}}_{k,\text{fa}} + \dot{n}^{\text{e}}_{k,\text{li}} \tag{22}$$

$$\dot{n}^{\text{e}}_{k,\text{bp}} = \dot{n}^{\text{i}}_{k,\text{lu}} \tag{23}$$

Here, subscript k denotes the possible substrate, i.e., free triclosan, glucuronide, and sulfate.

4 Simulation

4.1 Parameters

Once model equations are written, their parameters must be derived from experiments found in the literature, or estimated from correlation formulas such as in Eq. 10. Parameters for BPA were used in the PBPK model for TCS where values for TCS were not found.

Triclosan has been shown to be sulfonated and glucuronidated in human liver, and parameters of TCS are used regarding metabolism of the liver as shown in Table 2. Specific data for metabolism in human skin is lacking. Although the absorption mechanisms are different, metabolism parameters in the skin are lower than those for the liver; it was assumed that 20 percent of the corresponding parameters for the liver can be used for the skin reactions.

4.2 Operating Condition

The following operating condition are used in the model:

- Initial state: all are zero.

- Body Weight (BW): $0.25\,\text{kg}$ for rats and $73\,\text{kg}$ for human.

- Chemical dose: $0.1\,\text{g/kg}$ BW is supplied continuously for 1 hour in rats and 2 hours in humans.

- Consideration: relevant mass of protein in the skin is equal to the relevant mass of the protein of the liver $m_{\text{p,sk}} = m_{\text{p,h}}$.

4.3 Simulation Results

The simulations are carried out using MATLAB for both dermal and oral applications, using partition coefficient for BPA, but also using partition coefficients for TCS derived from Poulin's method. The results for TCS sulfate

---

[3] Assuming no transport limitation.

follow the same pattern as those for TCS glucuronide, and only the TCS glucuronide results are reported due to space constraints.

Figures 5 and 6 show the levels of TCS and TCS glucuronide using BPA coefficient and parameters of TCS found in the literature, or assumed. Organs like small intestine, muscles, and kidney show the same trend: a marked peak in the start due to the intake, while the elimination rate differs for these organs. The concentration of free triclosan is high in the liver and in the skin, compared to the other organs (lungs, fat, bones) because free triclosan is added in these two organs. In Figure 6 for both oral and dermal application, the trend of concentrations of glucuronide in organs is similar to that of free triclosan. The concentrations of the metabolites take relatively long time to settle down. Higher peaks of concentration of metabolites are present in the small intestine, in the liver and in the skin, where the transformation of triclosan takes time.

These results can be compared with the PBPK model for BPA in plasma from (Fowler, 2013) through oral exposure. Their study indicates a rapid increase in concentrations due to intake of the chemical, which goes to zero after some 8 hours. The maximum peak of concentration has the same order of magnitude for free triclosan in the case in Figure 5 for the small intestine and muscle which is the organs where most of the BPA is accumulated (Fowler, 2013). The time axis is not directly comparable, due to a different amount of intake of the chemical. In (Völkel et al., 2002), metabolites of BPA are formed when higher doses of bisphenol are taken in. The results of (Völkel et al., 2002) show that after oral application of low doses of BPA in humans, only a very small percentage of the dose of BPA is available for other bio transformation pathways, due to the rapid glucuronidation.

Similarly, Figures 7 and 8 show the level of TCS and TCS glucuronide based on the Poulin formulae for partition coefficient estimation (Poulin and Krishnan, 1995b). In Figure 7, the concentration in the kidney is higher than that of the liver in the free triclosan of using PCs of BPA; the elimination of TCS takes approximately 10 days. Also, the amount of free triclosan in bones shows a considerable difference from using the PCs of BPA. The time for elimination of the concentrations for other organs seems to take in the order of 2 days. In Figure 8, bones and fat have the highest concentration of TCS glucuronide. It is also interesting to compare the elimination time for TCS glucuronide. The results of simulation using Poulin's formula for PCs cannot be compared with results in the literature, for the lack comparable results. A high concentration of triclosan and TCS glucuronide is visible in the kidney and the small intestine, both with dermal and oral application.

5 Conclusions

In this study, a PBPK model for triclosan and its conjugates was developed, which indicates their concentration

https://doi.org/10.3384/ecp18153148

152

Proceedings of The 59th Conference on Simulation and Modelling (SIMS 59), 26-28 September 2018, Oslo Metropolitan University, Norway

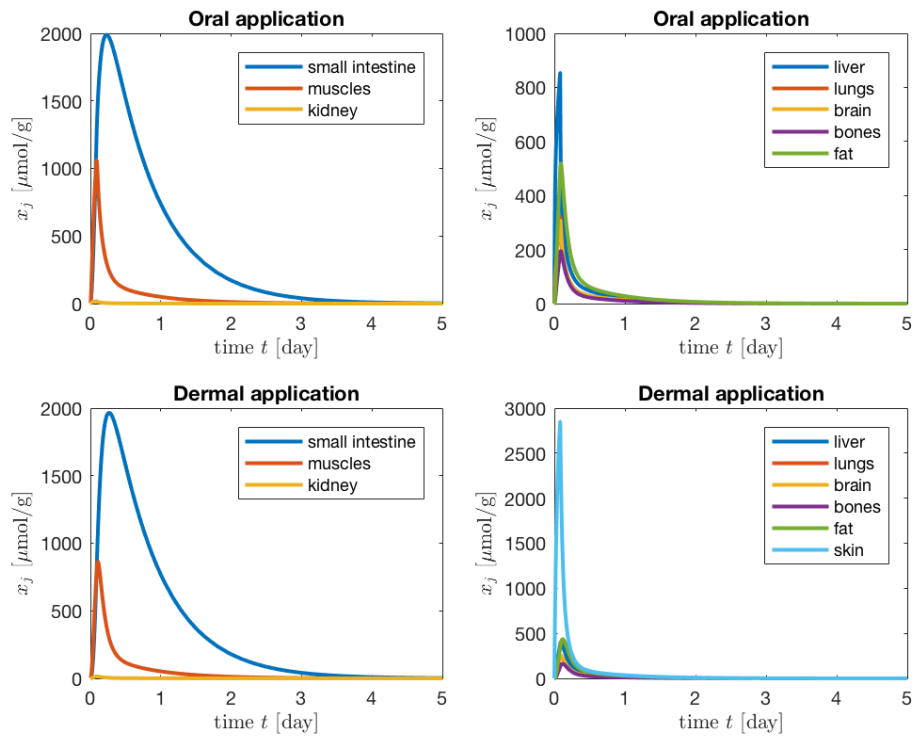**Figure 5.** Free Triclosan concentration simulated using BPA PCs.
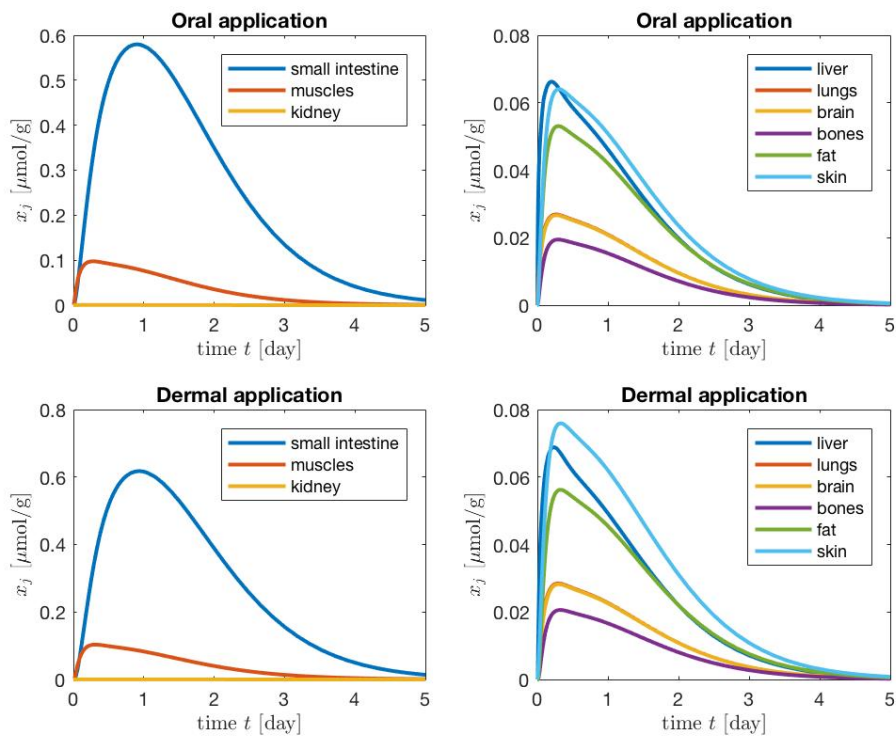
Figure 6. Glucuronide concentration of TCS simulated using BPA PCs.

https://doi.org/10.3384/ecp18153148

153

Proceedings of The 59th Conference on Simulation
and Modelling (SIMS 59), 26-28 September 2018,
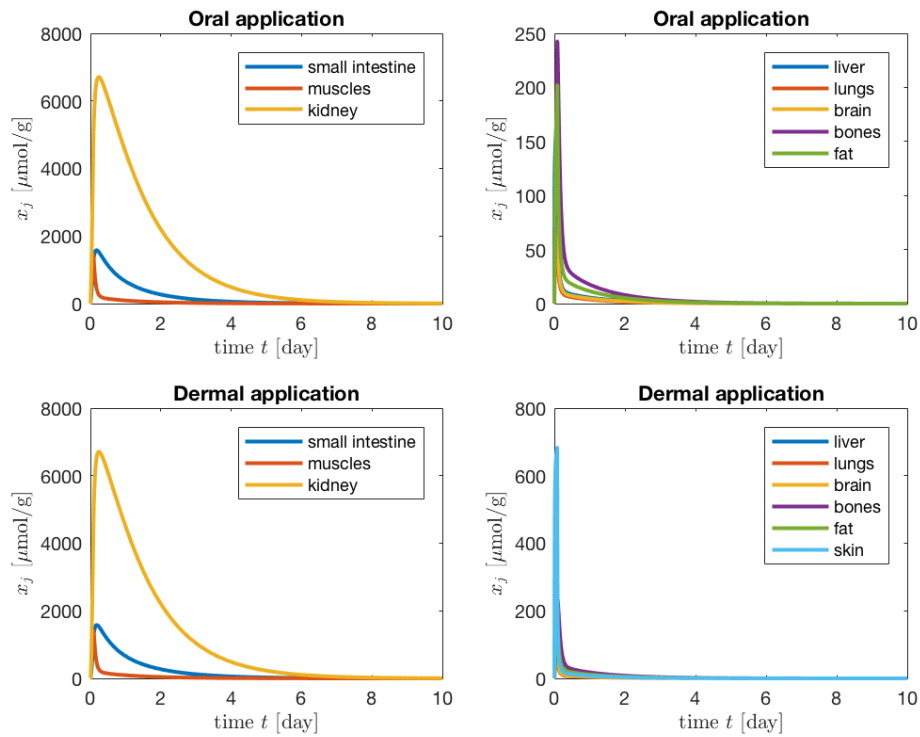Oslo Metropolitan University, Norway

Figure 7. Free Triclosan concentration simulated using formula of Poulin for PCs.
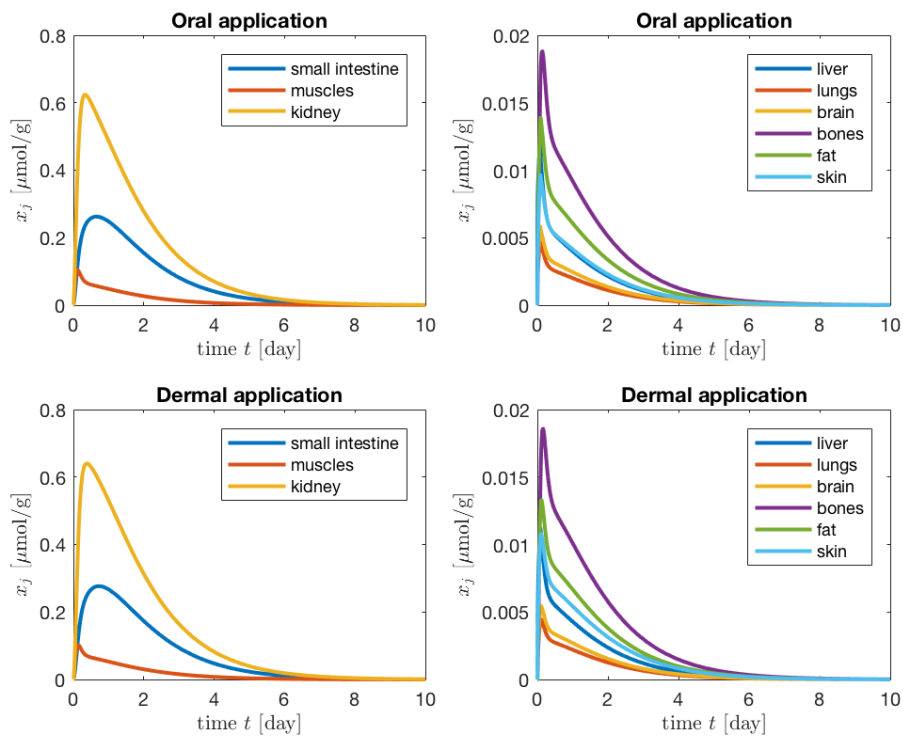
Figure 8. Glucuronide concentration of TCS simulated using formula of Poulin for PCs.

https://doi.org/10.3384/ecp18153148

154

Proceedings of The 59th Conference on Simulation
and Modelling (SIMS 59), 26-28 September 2018,
Oslo Metropolitan University, Norway

in organs of the human body. Organs such as muscles, fat, kidney, and liver have higher concentrations than the other organs, which seems reasonable and is in line with (Fang et al., 2010). The unavailability of parameters for Triclosan and simulation/experimental results for Triclosan in the literature makes it difficult to verify the results further at the moment.

References

Z. E. Barter, M. K. Bayliss, P. H. Beaune, A. R. Boobis, D. J. Carlile, R. J. Edwards, J. B. Houston, B. G. Lake, J. C. Lipscomb, O. R. Pelkonen, G. T. Tucker, and A. Rostami-Hodjegan. Scaling factors for the extrapolation of in vivo metabolic drug clearance from in vitro data: reaching a consensus on values of human microsomal protein and hepatocellularity per gram of liver. *Current Drug Metabolism*, 8(1): 33–45, January 2007.

Jerry L Campbell, Rebecca A Clewell, P Robinan Gentry, Melvin E Andersen, and Harvey J Clewell. Physiologically based pharmacokinetic/toxicokinetic modeling. In *Computational Toxicology*, pages 439–499. Springer, 2012.

Helen E Cubitt, J Brian Houston, and Aleksandra Galetin. Relative importance of intestinal and hepatic glucuronidation — impact on the prediction of drug clearance. *Pharmaceutical research*, 26(5):1073, 2009.

Andrea B Dann and Alice Hontela. Triclosan: environmental exposure, toxicity and mechanisms of action. *Journal of applied toxicology*, 31(4):285–311, 2011.

Jia-Long Fang, Robin L Stingley, Frederick A Beland, Wafa Harrouk, Debbie L Lumpkins, and Paul Howard. Occurrence, efficacy, metabolism, and toxicity of triclosan. *Journal of Environmental Science and Health, Part C*, 28(3):147–171, 2010.

Bruce A Fowler. *Computational toxicology: methods and applications for risk assessment*. Academic Press, 2013.

Aleksandra Konieczna, Aleksandra Rutkowska, and D Rachon. Health risk of exposure to bisphenol a (bpa). *Roczniki Państwowego Zakładu Higieny*, 66(1), 2015.

L. Kuepfer, C. Niederalt, T. Wendl, J.-F. Schlender, S. Willmann, J. Lippert, M. Block, T. Eissing, and D. Teutonico. Applied concepts in pbpk modeling: How to build a pbpk/pd model. *CPT: Pharmacometrics & Systems Pharmacology*, 5 (10):516–531, 2016.

Patrick Poulin and Kannan Krishnan. A biologically-based algorithm for predicting human tissue: blood partition coefficients of organic chemicals. *Human & experimental toxicology*, 14 (3):273–280, 1995a.

Patrick Poulin and Kannan Krishnan. An algorithm for predicting tissue: Blood partition coefficients of organic chemicals from n-octanol: Water partition coefficient data. *Journal of Toxicology and Environmental Health, Part A Current Issues*, 46(1):117–129, 1995b.

Anna Katharina Vingskes and Nicole Spann. The toxicity of a mixture of two antiseptics, triclosan and triclocarban, on reproduction and growth of the nematode caenorhabditis elegans. *Ecotoxicology*, pages 1–10, 2018.

Wolfgang Völkel, Thomas Colnot, György A Csanády, Johannes G Filser, and Wolfgang Dekant. Metabolism and kinetics of bisphenol a in humans at low doses following oral administration. *Chemical research in toxicology*, 15(10): 1281–1287, 2002.

Li-Quan Wang, Charles N Falany, and Margaret O James. Triclosan as a substrate and inhibitor of 3'-phosphoadenosine 5'-phosphosulfate-sulfotransferase and udp-glucuronosyl transferase in human liver fractions. *Drug Metabolism and Disposition*, 32(10):1162–1169, 2004.

Min Ye, Swati Nagar, and Ken Korzekwa. A physiologically based pharmacokinetic model to predict the pharmacokinetics of highly protein-bound drugs and impact of errors in plasma protein binding. *Biopharmaceutics & Drug Disposition*, 37(3):123–141, 2016.

P Zhao, L Zhang, JA Grillo, Q Liu, JM Bullock, YJ Moon, P Song, SS Brar, R Madabushi, TC Wu, et al. Applications of physiologically based pharmacokinetic (pbpk) modeling and simulation during regulatory review. *Clinical Pharmacology & Therapeutics*, 89(2):259–267, 2011.

Xiaomei Zhuang and Chuang Lu. Pbpk modeling and simulation in drug research and development. *Acta Pharmaceutica Sinica B*, 6(5):430–440, 2016.

https://doi.org/10.3384/ecp18153148

155

Proceedings of The 59th Conference on Simulation and Modelling (SIMS 59), 26-28 September 2018, Oslo Metropolitan University, Norway